Processes of faulting in jointed rocks of Canyonlands National Park, Utah

Jason M. Moore* } *Geomechanics–Rock Fracture Group, Department of Geological Sciences 172,*
Richard A. Schultz† } *Mackay School of Mines, University of Nevada, Reno, Nevada 89557*

ABSTRACT

Detailed studies of 11 segmented normal faults from five grabens in the Needles District of Canyonlands National Park, Utah, demonstrate key processes in the growth, linkage, and evolution of grabens. Field observations and stereophotogrammetry reveal a ubiquitous asymmetry in cross-sectional geometry, based on distinct map patterns of graben-bounding faults, rollover anticlines with attendant joint dilation, footwall uplift with joint closure, and spoon-shaped graben floors. Master and antithetic faults across Devils Lane and several other grabens are defined quantitatively by the displacement distributions along the faults. Two-dimensional shape parameters that characterize the displacement profiles indicate that inelastic processes such as changes in fault frictional strength influence strain accumulation along the faults. The degree of graben asymmetry increases systematically with distance from the Colorado River; greater symmetry is associated with locally greater age and/or strain of grabens nearer the river. Scatter in plots of maximum displacement vs. fault length was attributed previously to linkage of fault segments alone but is here shown to correlate additionally with distance from the Colorado River and, therefore, to spatial strain gradients within the graben array. Extensional strain across the fault array, accumulating at rates of perhaps 1.5 to 2 cm/yr or 10^{-14} to 10^{-13} s^{-1}, is accommodated at depth by salt flow and formation of reactive salt diapirs beneath the grabens and was probably initiated when the Colorado River had cut sufficiently deep into the section for active salt diapirism to commence.

INTRODUCTION

Faulting in jointed rocks involves slip along frictionally weak surfaces, mechanical interaction between faulted parts of the joints, and inelastic strain in the stepover regions between them (Fig. 1). Earthquakes typically nucleate along fracture surfaces at depth (e.g., Scholz, 1990; Roberts and Yielding, 1994) and propagate vertically and laterally as slip patches (e.g., Martel and Pollard, 1989; Cowie and Shipton, 1998), eventually producing large, crustal-scale faults having sizable geologic offsets (Cowie and Scholz, 1992a) comparable to the faults in Canyonlands. The mechanism of faulting in Canyonlands grabens, developed in jointed sandstones, is the same as that documented in many areas in crystalline rocks such as granite in which faults nucleate on preexisting joints; in both rock types, faults increase in length by mechanical interaction and linkage of slipped joints (e.g., Martel, 1990; Martel and Boger, 1998). However, the Canyonlands grabens differ in that (1) only parts of some joints have slipped and (2) the grabens are developed at the Earth's surface and thus preserve key details of the processes of slip-patch propagation along weak joints.

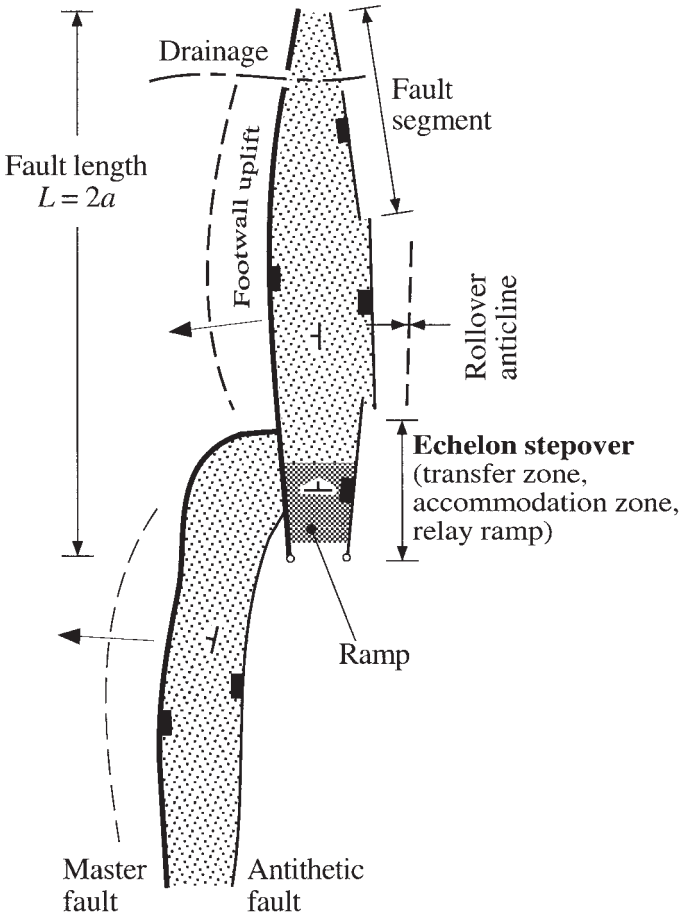

Figure 1. Definition of terms used in this study of segmented normal faults. Ramp of flexed strata (darker pattern) bridges fault terminations (= fault tips [circles]) of graben-bounding faults. Specific structures and terminology within the stepover region between echelon grabens depend on polarity of master fault for each graben.

Individual normal faults can combine in three dimensions to create mechanically, aesthetically, and economically important patterns. Parallel normal faults can overlap partially, forming echelon geometries analogous to those documented for dilatant cracks (Pollard and Aydin, 1988) and strike-slip faults (Aydin and Nur, 1985). Within the overlap, or stepover region (Fig. 1), large stress and strain gradients occur (Willemse et al.,

*Present address: Science Applications International Corp. (SAIC), P.O. Box 93838, Las Vegas, Nevada 89193-3838.
†Corresponding author; e-mail: schultz@mines.unr.edu.

GSA Bulletin; June 1999; v. 111; no. 6; p. 808–822; 13 figures; 2 tables.

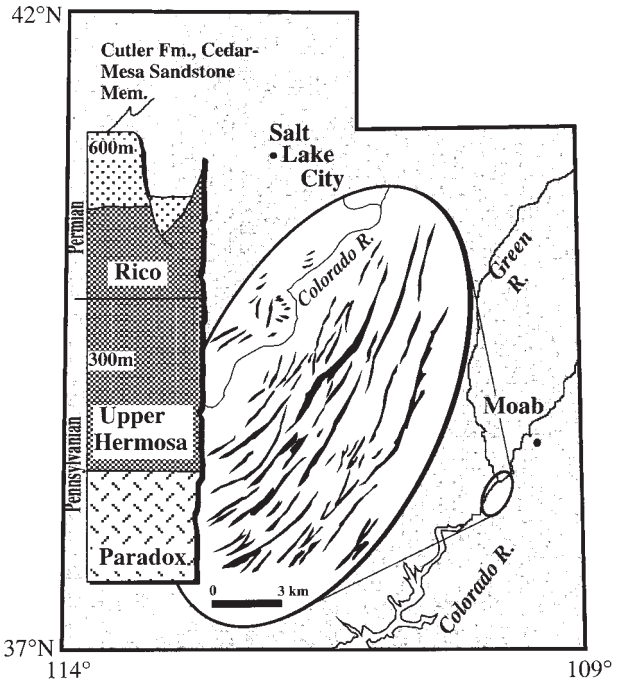

Figure 2. Location of graben system in the Needles District of Canyonlands National Park, Utah, after Schultz and Moore (1996). Insets show stratigraphic section from Lewis and Campbell (1965) and generalized graben locations (within ellipse) from Trudgill and Cartwright (1994).

1996; Crider and Pollard, 1998). Here, strata are flexed and faulted into patterns known variously as relay ramps, transfer zones, and accommodation structures or by other terms (Larsen, 1988; Ebinger, 1989; Bruhn et al., 1990; Morley et al., 1990; Gudmundsson and Bäckström, 1991; Peacock and Sanderson, 1994; Mack and Seager, 1995; Moustafa, 1997; Faulds and Varga, 1998). These areas define pathways for sediment transport (Anders and Schlische, 1994) and structural traps that are of importance in large oil and gas fields throughout the world (Morley et al., 1990; Jackson and Vendeville, 1994; Stewart et al., 1996).

Parallel, noncoplanar normal faults that completely overlap, with small separations relative to their lengths, define grabens that commonly exhibit a greater amount of vertical stratigraphic offset (throw) on one (master) fault than on the other (antithetic) fault. Such asymmetric grabens (Gibbs, 1984; Rosendahl, 1987; Groshong, 1989; Jackson and White, 1989) can display a rich assemblage of topographic features (Davison, 1994) such as footwall uplift (Weissel and Karner, 1989) and hanging-wall subsidence (Gudmundsson and Bäckström, 1991). These topographic elements increase in amplitude from zero at the graben terminations to maximum values near the middle regions of the fault, tracking the shape of the displacement distribution and location of maximum offset, D_{max} (e.g., Barnett et al., 1987; Pollard and Segall, 1987; Walsh and Watterson, 1987; Bürgmann et al., 1994).

Scaling relationships between the maximum value of displacement along a fault and its map length have been refined during the past decade (Peacock and Sanderson, 1996; Clark and Cox, 1996; Cartwright et al., 1995, 1996; Bürgmann et al., 1994; Cowie and Scholz, 1992b; Walsh and Watterson, 1987). Discrepancies over specific values for the scaling-law parameters result in part from insufficient data from faults of differing scales, amounts of linkage, and rock types. Whereas knowledge of only D_{max} may be sufficient to discuss displacement vs. length scaling relationships at a general level (e.g., Cowie and Scholz, 1992b; Schultz, 1997), profiles recording displacement variations along the length of the fault are required to understand and predict fault-slip behavior (e.g., Cowie and Scholz, 1992c; Scholz et al., 1993; Bürgmann et al., 1994; Peacock and Sanderson, 1996; Dawers et al., 1993; Dawers and Anders, 1995; Caskey et al., 1996) and ramp kinematics (Schultz and Moore, 1996; Cartwright and Mansfield, 1998).

We report results from the unusually well preserved grabens in Canyonlands National Park that provide insights into displacement accumulation and strain accommodation along closely spaced normal faults and their interactions with subjacent evaporites that flow in a ductile manner. We document a pervasive and important asymmetry in the cross-sectional form of the grabens, in contrast to prior suggestions of symmetric structures (McGill and Stromquist, 1979; Cartwright et al., 1996), and use concepts of balanced cross sections and salt tectonics (e.g., Jackson et al., 1994; Jackson, 1995) to interpret these structures. We measure displacement distributions along graben-bounding normal faults and use two-dimensional parameters for characterizing the shapes of the displacement distributions. These segmented echelon normal faults follow a general displacement vs. length scaling relationship (Cartwright et al., 1995) comparable to many other fault sets (e.g., Cowie and Scholz, 1992b; Clark and Cox, 1996). We demonstrate that D_{max} varies systematically by a factor of four across the Needles District (normal to strike) and suggest that segment linkage may be one of several factors in the scaling relationships (compare with Cartwright et al., 1995, 1996). While the Canyonlands grabens are apparently forming in response to localized stress perturbations and in association with ductile flow of subjacent evaporites, their general characteristics are surprisingly similar to those of both smaller and larger grabens elsewhere (e.g., Larsen, 1988; Ebinger, 1989; Jackson and White, 1989; Bruhn et al., 1990; Morley et al., 1990; Gudmundsson and Bäckström, 1991; Peacock and Sanderson, 1994; Trudgill and Cartwright, 1994; Mack and Seager, 1995; Bruhn and Schultz, 1996) although their specific geometries are strongly influenced by the strength anisotropy associated with the preexisting joint set (e.g., McGill and Stromquist, 1979).

GEOLOGIC BACKGROUND

The Needles District fault zone defines an arcuate, northwest-trending system of grabens (McGill and Stromquist, 1979; Trudgill and Cartwright, 1994; Cartwright et al., 1995; Schultz and Moore, 1996). The grabens occur from the confluence of the Green and Colorado Rivers in the north to Gypsum Canyon (outside the study area) in the south (Nuckolls and McCulley, 1987; Fig. 2). Most of the grabens occur to the east of the Colorado River for at least 5 km; a few grabens occur to the west, including Surprise Valley (Fig. 3). In this paper we focus on grabens along a traverse in the northern part of the region. The grabens range from about 100 m to 6 km in length and are generally spaced 700 m to 1000 m apart. Widths at the surface range from less than 100 m to more than 400 m; graben depths (exposed stratigraphic offsets along the faults) range from less than 25 m to more than 100 m (McGill and Stromquist, 1975; Cartwright et al., 1995). Graben floors are draped by a combination of Quaternary colluvial, eolian, and alluvial sediments (Biggar, 1986) that creates a smooth, subhorizontal surface. The sheer walls and flat floors of these grabens make them popular tourist attractions.

The grabens have challenged geologists at least since the early twentieth century (Harrison, 1927; Baker, 1933). The tributary canyons near the grabens were cut by the Colorado and Green Rivers, resulting in erosion and localized unloading of the strata overlying the Pennsylvanian Paradox Member of the upper part of the Hermosa Formation (Lewis and Campbell, 1965) during Pleistocene to Holocene time (Hunt, 1969; McGill and Stromquist, 1974). The grabens deform an ~460-m-thick section of clastic

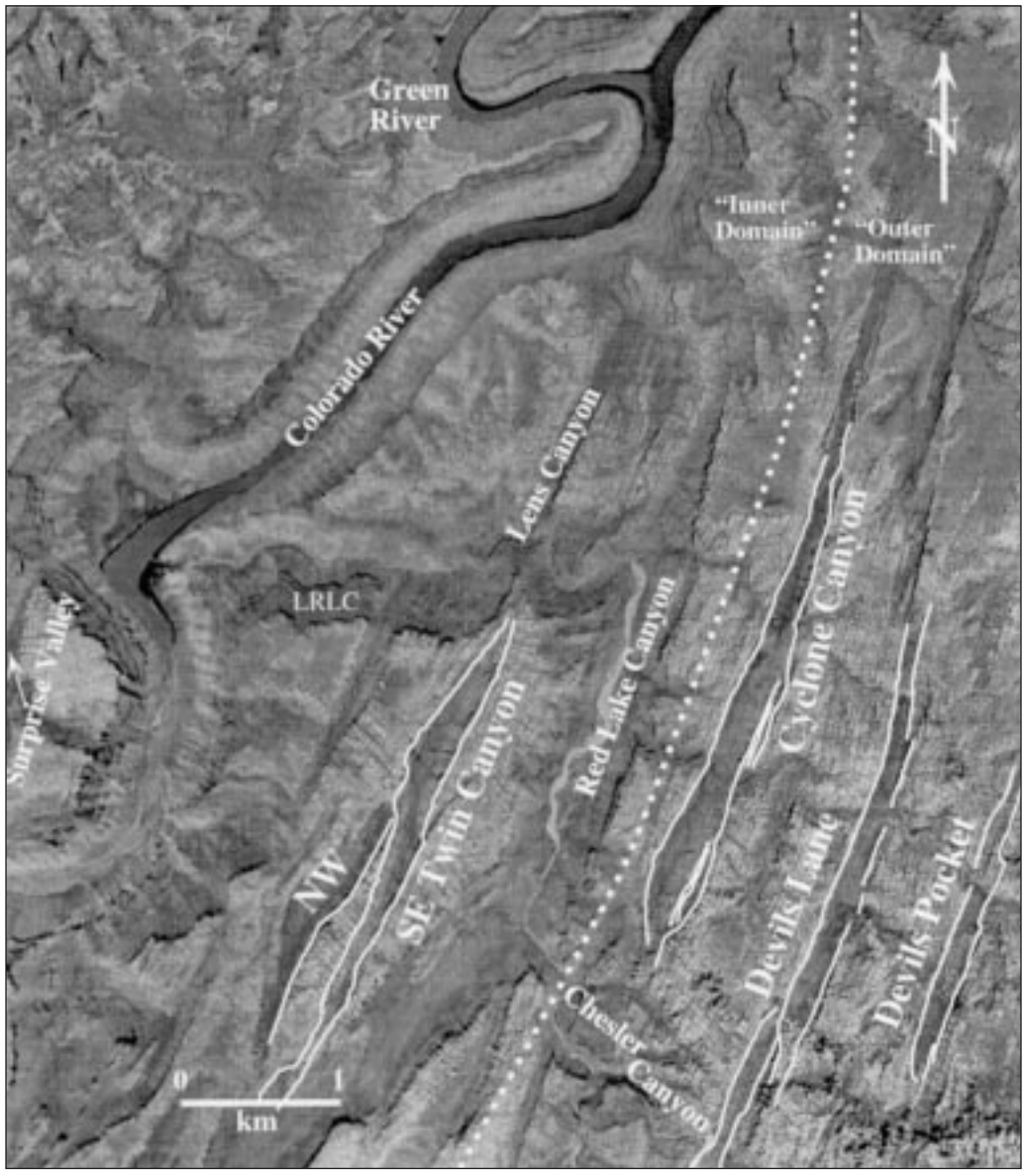

Figure 3. U.S. Geological Survey aerial photograph (1:40 000) of part of the Needles District graben system, centered near 38°N, 110°W. Grabens (named in figure) are curvilinear depressions filled with Quaternary sediments (darkened by vegetation). Horsts are typically capped by white Cedar Mesa Sandstone. Pervasive joints are generally parallel or nearly orthogonal to grabens. Grabens measured and discussed in this paper are shown and annotated; profiles given in Figure 5. Spanish Bottom and Cataract Canyon (not shown) are located southwest of Surprise Valley. LRLC—Lower Red Lake Canyon.

sedimentary rocks that overlie gypsum and other evaporites in the Paradox Member (Fig. 2). The brittle sequence exhibits a gentle regional slope of about 4° to the west, or less, down the flank of the older Monument upwarp (Elston et al., 1962; Stevenson and Baars, 1986). Downdip sliding of the sequence and/or flow of subjacent Paradox evaporites is thought to have formed the grabens in the overlying rocks (e.g., Baker, 1933; Lewis and Campbell, 1965; McGill and Stromquist, 1975; Huntoon, 1982; Trudgill and Cartwright, 1994; Cartwright et al., 1995). Unloading of the end of the clastic sequence at the Colorado River gorge (Harrison, 1927) and formation of the Meander anticline (Potter and McGill, 1978; Huntoon, 1982) at the gorge by salt diapirism (Jackson and Vendeville, 1994) imply that Needles District grabens nucleated first near the river (likely beginning with Red Lake Canyon: Biggar, 1986) and decrease in age eastward (e.g., McGill and Stromquist, 1979; Huntoon, 1982; Biggar, 1986; Ely, 1987). Our independent results support this scenario.

Past and present deformation due to salt flow is common in southeastern Utah; there are several salt-cored anticlines in the region (Witkind, 1994) such as the Meander anticline along the Colorado River and others along smaller canyons (Potter and McGill, 1978; Huntoon, 1982). Deformation of Quaternary sediments to the north in Salt Valley (Cruikshank and Aydin, 1995) and minor Quaternary salt-related slip of the Moab fault (Olig et al., 1996) and other nearby faults (Wong et al., 1996) suggest contemporary ex-

Figure 4. Oblique aerial photograph showing representative grabens and prefaulting jointed rock mass. Rectangular blocks in center of photograph are bounded by prominent joint sets, one trending northeast and the other trending northwest. View to north. DL—Devils Lane graben (width, ~200 m); CC—Cyclone Canyon; RLC—Red Lake Canyon. Photograph by J. M. Moore.

tension associated with salt flow. Within the Needles District, evidence cited for continuing extension includes possible topple failures (Adhikary et al., 1997) of vegetated slabs (Trudgill and Cartwright, 1994) and dilating cracks along many graben walls (swallow holes: Ely, 1987; Biggar and Adams, 1987) and near their terminations (Cartwright and Mansfield, 1998). However, it is interesting that the Needles District fault zone is not seismogenic (Wong et al., 1987, 1996) although aseismic creep along some faults has been reported or inferred during historic times (Lewis and Campbell, 1965; G. E. McGill, 1997, personal commun.).

METHODS

Field Investigation

Our field work focused on understanding the three-dimensional geometry of the grabens, their relationship to the prominent joint sets (Fig. 4), and the implications for salt involvement and mechanical behavior of the structures. We used Lewis and Campbell's (1965) stratigraphy (Fig. 2) rather than more common stratigraphic conventions (Baars, 1962; Huntoon et al., 1982) in order to facilitate the identification of stratigraphic offsets across the grabens. Lewis and Campbell's units are readily identified from a distance (see also the reevaluation of Baars's nomenclature by Loope [1984, 1985]) and, therefore, are more convenient for field-based structural analysis (McGill and Stromquist, 1979). Previous structural investigations of the grabens, including McGill and Stromquist's seminal works (1974, 1979) as well as later studies (Trudgill and Cartwright, 1994; Cartwright et al., 1995, 1996), follow this convention, and differences in terminology are not important to the present study. The basal Paradox Member of the Hermosa Formation is composed of unmistakable gray and white evaporites. These are exposed locally in tributary canyons as emergent salt diapirs. The upper part of the Hermosa Formation is a series of thick-bedded limestones, shales, and sandstones that form steep gray cliffs. The overlying Rico Formation consists of thinly bedded limestones, shales, and sandstones that form steep, stair-stepping red cliffs. Finally, the Cedar Mesa Sandstone Member (Cutler Formation, Permian) is composed of interbedded tan sandstones and red siltstones, and fine-grained sandstones (Loope, 1984); this unit weathers into toadstool-like blocks and provides a distinctive stratigraphic marker and cap rock in grabens such as Devils Lane.

Stereophotogrammetry

Data collected from aerial photographs were used to confirm and quantify key stratigraphic relationships recognized in the field. Our laboratory study used a Kern PG-2 stereophotogrammetric plotter to determine both relative and absolute elevation data. This instrument allowed us to calculate the scarp height of the graben-bounding faults with ±2 m relative precision (Messerich, 1989; Banks, 1982). Scarp relief (cap rock to graben floor) was measured at regular 100 m intervals along each fault; in the Needles District, relief is a close approximation of structural offset (McGill and Stromquist, 1979; Trudgill and Cartwright, 1994; Cartwright et al., 1995).

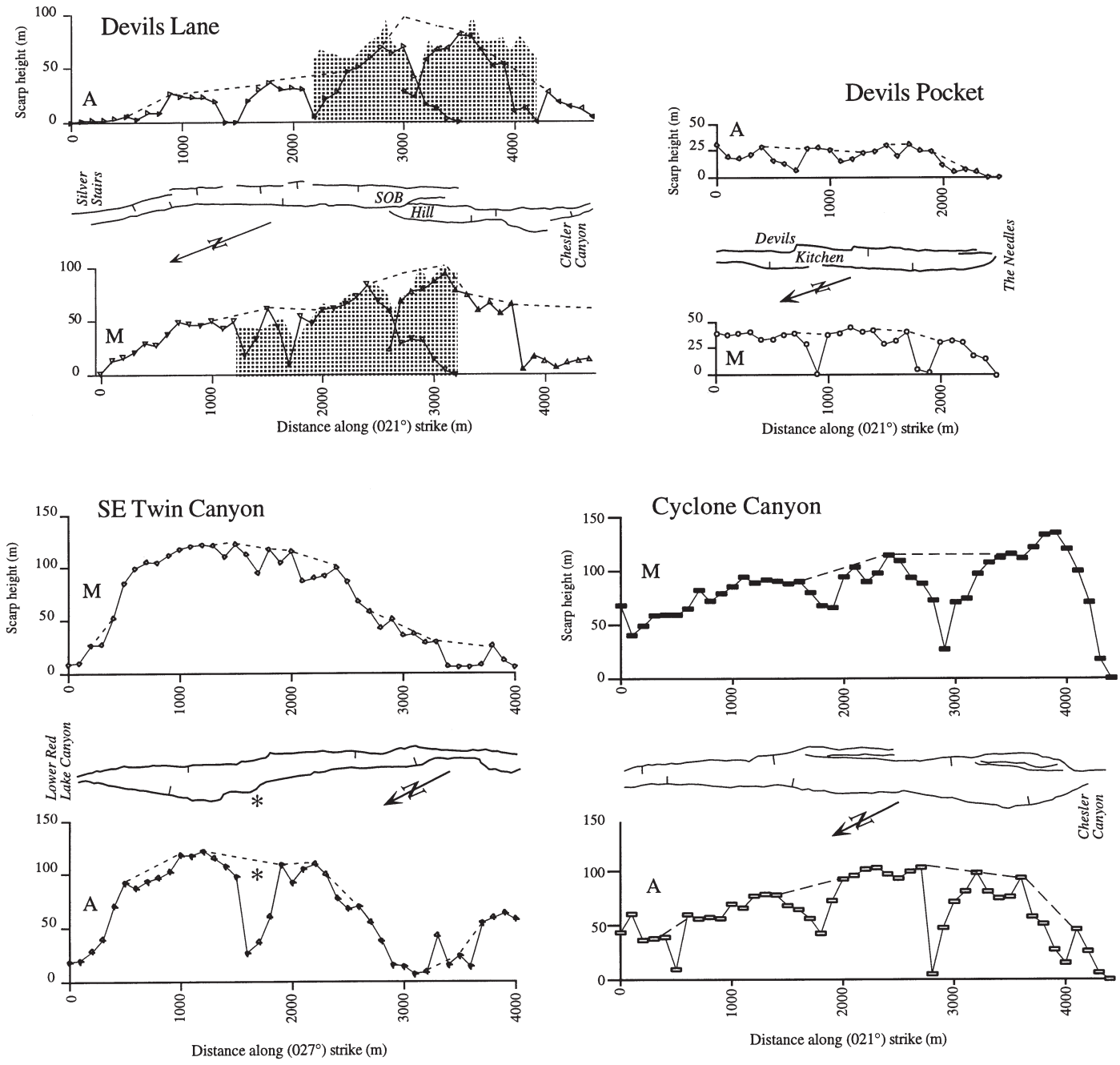

Figure 5. Topographic profiles for Devils Lane, Devils Pocket, southeast Twin Canyon, and Cyclone Canyon grabens (scale constant for comparison; vertical exaggeration 10:1). Profiles for adjoining, facing faults in each graben are grouped in pairs (thick solid lines); map traces of graben-bounding faults (thin solid lines) are shown in center of each profile pair. M—master faults, A—antithetic faults. Prominent drops within the profiles are typically produced by preexisting drainages and erosion, but may be the product of fault linkage or fault interaction in some cases. Dashed outlines approximate displacement profiles, corrected for drainages and other nonstructural relief, corresponding to strike projections of vertical offset. Shaded regions show previous measurements for Devils Lane reported by Trudgill and Cartwright (1994). Asterisks in southeast Twin Canyon antithetic fault profile and accompanying map show point of intersection of southeast Twin Canyon (the main graben) with abutting northwest Twin Canyon (Fig. 3).

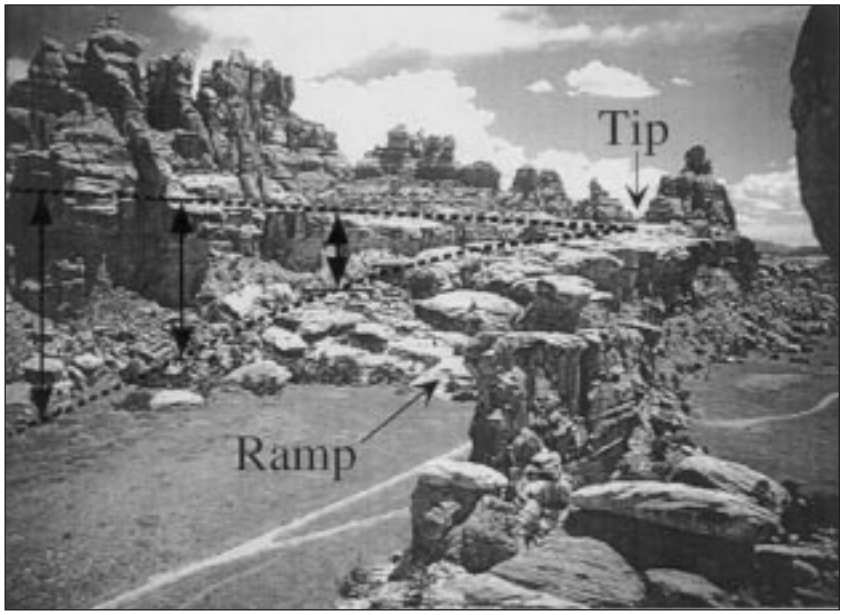

Figure 6. Southeast view of ramp and stepover at the southern end of northern Devils Lane graben (at S.O.B. Hill). Offset and light-colored toadstools of Cedar Mesa Sandstone Member define the near-tip displacement gradient (arrows) of the graben-bounding normal fault as the displacement tapers to zero at the fault termination. Submeter displacement occurs for more than 100 m beyond the ramp, toward the notch on the skyline (arrow labeled "tip"). Graben width at base of ramp is ~100 m.

The topographic profiles record displacement variations for the entire length of the fault that can be normalized to total fault length and maximum displacement. Our aerial photograph–based measurements generally compare well with values along the central part of Devils Lane graben reported previously by Trudgill and Cartwright (1994; shaded areas in Fig. 5). Details of the technique are given in Appendix 1. The grabens selected for our work have well preserved, nearly vertical walls (in the upper 100 m of the section) and are between 2 and 5 km long.

RESULTS AND DISCUSSION

Field Relationships

At the surface, most graben walls are nearly vertical, but in well-developed, deep drainages (e.g., Lower Red Lake Canyon), the fault dips decrease to ~75°–85° (McGill and Stromquist, 1974, 1979; Stromquist, 1976; Trudgill and Cartwright, 1994). This interpretation is supported by independent observations of two colluvium-filled fault fissures dipping ~70° about 300 m below the graben floor near Cataract and Cross Canyons (Ely, 1987). Recent workers (Cartwright et al., 1995, 1996) have postulated that the graben-bounding faults remain vertical to subvertical for 400–500 m from the surface (depth to the Paradox evaporites); however, this geometry is suspect because few, if any, grabens are exposed vertically for 500 m in cross section in the Needles District (Lewis and Campbell, 1965; Huntoon et al., 1982). We reconfirmed McGill's observations by visiting the same exposures with him in May 1997, noting that all graben-bounding normal faults observable in cross section dip at 75° or less at some depth below the surface.

Faults in the study area are almost exclusively normal. Slickensides are poorly preserved on the fault surfaces; where slickenlines are found, rakes are approximately vertical (90°), an indication of pure dip-slip displacement. Tool marks and casts of grooves in fault-filling calcite mineralization in several localities (especially near ramps in the young and well-preserved Devils Pocket grabens) indicate that the faults were in frictional contact when they slipped, in contrast to some previous suggestions. Subsequent opening and/or slip events are associated with calcite deposition along many of the faults. Joints that did not slip and become faults are not commonly found associated with calcite coatings in the areas investigated. Other faults with reverse displacement are documented at deep structural levels (300 m down from the surface) close to Cataract Canyon (Ely, 1987), in the core of the Meander anticline (Huntoon, 1982) and within the Rico Formation near Chesler Canyon (observations by J. Moore).

Displacement Distributions

Displacement distributions for representative grabens are shown in Figure 5. Devils Lane graben, probably the best-studied graben structure in the Needles District (e.g., McGill and Stromquist, 1979; Trudgill and Cartwright, 1994), is composed of two closely spaced, right-stepping, echelon grabens; the stepover between them is located at S.O.B. Hill. The Devils Lane system is composed of four main fault segments, all of which interact mechanically—a conclusion inferred, in part, from relay ramps of flexed strata and cross faults in the stepover region between the faults (Trudgill and Cartwright, 1994). Strike projections of vertical offset (Fig. 5) demonstrate tapered displacement profiles near fault terminations (where exposed or preserved) and maximum values of displacement located near the fault midpoints. In Devils Lane, steeper displacement gradients for the individual fault segments occur where they approach each other, near the stepover, implying significant mechanical interaction (Willemse et al., 1996) and displacement transfer between the segments (Peacock and Sanderson, 1994; Willemse, 1997). Changes in the frictional properties along the fault, spatial gradients in the stress field, mechanical interaction between adjacent fault segments, inelastic deformation near fault tips, and variations in host-rock elastic modulus can produce asymmetrical, skewed slip distributions (Bürgmann et al., 1994) similar to those observed along individual fault segments in Devils Lane.

The intersection of the dipping ramp and vertical fault wall (Fig. 6) graphically reveals a spectacular near-tip displacement profile along the antithetic fault of northern Devils Lane graben. Recent field work (Schultz and Moore, 1996) has shown that graben-bounding faults in the Needles District can exhibit displacements of 1–2 m extending perhaps hundreds of meters

TABLE 1. FAULT DISPLACEMENT DATA FOR DEVILS LANE GRABEN PAIR

Fault*	D_{avg} (m)	D_{max} (m)	Length L (m)	D_{max}/L	D_{avg}/D_{max}
NW	38.8	82.9	3200	2.9×10^{-2}	0.47
NE	22.7	69.2	3500	2.0×10^{-2}	0.33
SW	47.5	93.3	1800	5.2×10^{-2}	0.51
SE	37.4	80.5	1700	4.7×10^{-2}	0.46
W†	47.4	108.5	4500	2.4×10^{-2}	0.44
E	31.0	97.5	4700	2.1×10^{-2}	0.32

*Faults labeled NW and NE define north part of graben; faults labeled SW and SE define south part of graben. W indicates the composite fault composed of linked master faults (i.e., NW and SW); E indicates the composite fault composed of linked antithetic faults (i.e., NE and SE).
†W composite fault defined by linkage of master faults; E fault, linked antithetic faults.

TABLE 2. FAULT DISPLACEMENT DATA FOR OTHER GRABENS

Fault*	D_{avg} (m)	D_{max} (m)	Length L (m)	D_{max}/L	D_{avg}/D_{max}
DP SE	18.7	30.5	2400	1.3×10^{-2}	0.61
DP NW	29.4	43.9	2500	1.8×10^{-2}	0.67
CC NW	65.5	103.0	4400	2.3×10^{-2}	0.64
CC SE	83.5	135.3	4400	3.1×10^{-2}	0.62
SE TC SE	73.2	121.6	3600	3.4×10^{-2}	0.60
SE TC NW	65.2	121.0	3600	3.4×10^{-2}	0.54
NW TC SE	84.4	129.8	2200	5.9×10^{-2}	0.65

*DP—Devils Pocket graben, SE and NW faults; CC—Cyclone Canyon graben; TC—Twin Canyon graben (SE and NW-bounding faults).

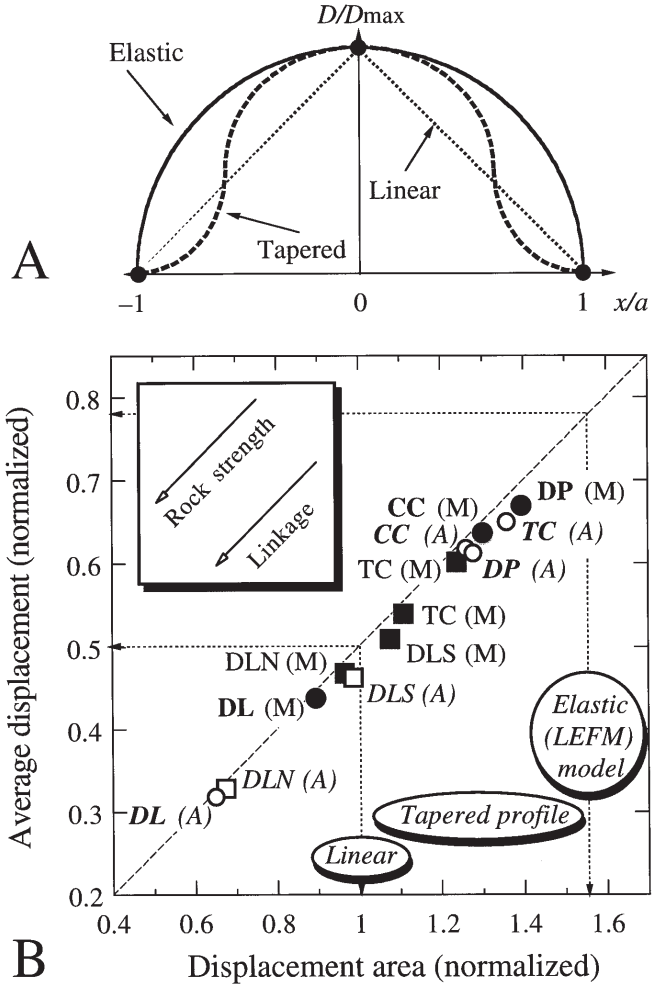

Figure 7. (A) Ideal displacement distributions (elastic, tapered, or linear) normalized to maximum displacement (*y*-axis) and fault length (*x*-axis). (B) Plot of two-dimensional fault-displacement parameters for Canyonlands graben faults showing various degrees of implied inelasticity (for the nonelliptical profiles) and taper (smooth decrease in displacement toward zero at the tip; $0.5 < D_{avg} < 0.77$; vertical axis of plot) of the displacement distributions; data from Tables 1 and 2. Master faults—filled symbols and bold labels. Antithetic faults—open symbols. Linked faults—circles and italic labels. Individual segments—squares. DL—Devils Lane graben; CC—Cyclone Canyon; DP—Devils Pocket graben; TC—southeast Twin Canyon graben and adjoining northwest Twin Canyon master fault; N—north; S—south.

beyond the ends of classically defined ramps. Such gently tapered distributions, reminiscent of slip patches along joints (Martel and Pollard, 1989), are prima facie evidence for inelastic deformation or nonuniform loading of faulted rock (Bürgmann et al., 1994). The nearly asymptotic near-tip profile is consistent qualitatively with a cohesive-zone model providing for inelastic deformation and finite stress magnitudes at the fault tips (Cowie and Scholz, 1992c; Scholz et al., 1993; Carter and Winter, 1995; Martel, 1997) and spread of patches of normal-fault slip along weak joint surfaces.

Displacement vs. Length Scaling

Interaction and/or linkage of individual segments can create a composite slip distribution resembling that of a single fault (Dawers and Anders, 1995; Willemse et al., 1996; Fig. 5), although the value for the maximum displacement along the composite, interacting fault array (composed of closely spaced fault segments) is somewhat less than that of an equivalent single continuous surface (Segall and Pollard, 1980; Willemse, 1997). Cartwright et al. (1995, 1996) suggested that large variations in displacement/length (D_{max}/L) ratios of individual segments could be attributed to a disequilibrium between accumulation of displacement along discontinuous fault segments and their propagation (e.g., Peacock and Sanderson, 1996). This phenomenon would imply that certain fault structures do not maintain a critical aspect ratio during slip, as implied in some solutions of cohesive-zone models of fault growth (Cowie and Scholz, 1992c; Scholz et al., 1993).

Displacement data measured for Devils Lane graben (Fig. 5) are given in Table 1 for the individual (unlinked) fault segments and for the summed (linked) fault sets. D_{max}/L ratios for the unlinked fault segments range from 2.0×10^{-2} to 5.2×10^{-2}, varying by less than a factor of three. The summed faults define D_{max}/L ratios of 2.1×10^{-2} to 2.4×10^{-2}; the ratios decrease relative to the unlinked segments because linkage increases fault length relatively faster than the total displacement, resulting in a flatter displacement profile. The value of D_{max}/L for the composite Devils Lane faults is comparable (within a factor of two) to that for the individual fault segments. We infer that other processes in addition to segment linkage are required to fully account for factor-of-five variations in the displacement vs. length scaling relationships demonstrated for Canyonlands grabens (Cartwright et al., 1995). However, fault interaction and linkage do appear to shift the D_{max}/L ratio to somewhat smaller values, during the growth process, relative to those appropriate for the fault segments.

Average Displacement and Displacement Area

Whereas D_{max} represents a sample of only one point along a displacement distribution, two-dimensional parameters such as average displacement D_{avg} (Dawers et al., 1993), or displacement area D_{area}, represent a

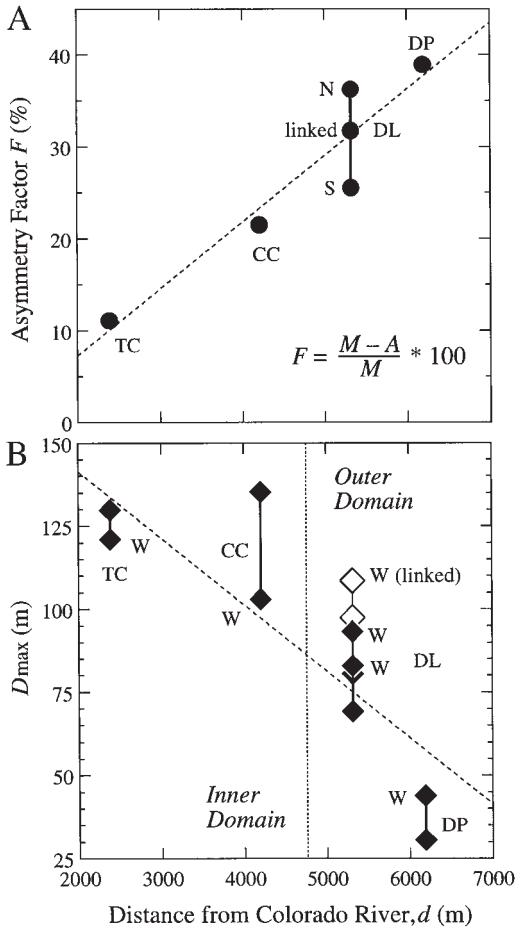

Figure 8. Variation in graben properties across the Needles District. (A) Increase in degree of graben asymmetry with distance from the Colorado River. Asymmetry factor *F* calculated from displacement areas of master fault (*M*) and antithetic fault (*A*). Data for Devils Lane graben system (DL) shown as linked or as individual north (N) and south (G) grabens. Least-squares fit suggests a good correlation, $F = 0.007d - 7.183$, $r^2 = 0.880$. DL—Devils Lane echelon graben pair, linked; N—northern Devils Lane graben; S—southern Devils Lane graben. (B) Systematic decrease in the maximum fault displacement D_{max} with distance from Colorado River. Least-squares fit suggests $D_{max} = -0.02d + 181$, $r^2 = 0.734$. Inner and outer domains associated with distinct and consistent facing directions for master faults (Fig. 3); faults on western sides of grabens (W) and unequal D_{max} values for same graben identify facing directions of master faults (west dipping, inner domain; east dipping, outer domain).

more stable and informative characterization of the shape of the distribution. In particular, D_{avg}/D_{max} can reveal differences between an ideal elastic profile, linearly varying profiles (Bürgmann et al., 1994), and profiles with various degrees of taper related to cohesive-zone models of fault terminations (Cowie and Scholz, 1992c; Martel, 1997; Willemse and Pollard, 1998). On the other hand, displacement area (calculated by multiplying the sum of the displacement measurements by the distance between each measurement) is an even more elegant description of fault slip because it explicitly reflects the size (length and displacement) of the fault. Displacement area can be related to the work done by applied loads (e.g., Cowie and Scholz, 1992a) to create the fault surface area. Both of these two-dimensional quantities are necessary for the quantitative restoration of regional strains due to faulting (e.g., Gauthier and Angelier, 1985; Marrett and Allmendinger, 1990).

Appropriately normalized values of the average displacement, along with normalized area of displacement (Table 2), can succinctly recover important details of the displacement distribution along isolated or linked faults (e.g., Cowie and Scholz, 1992c). We convert the displacement profiles to dimensionless form by dividing the measured displacement values D by D_{max} and relating the horizontal position of the displacement measurement along the fault, x, to the total fault length, $2a$, where $-1 \le x/a \le 1$ (e.g., Bürgmann et al., 1994; Moore, 1997; Fig. 7a). By removing the effect of variable fault length, the Canyonlands slip displacement distributions can be compared directly to ideal shapes predicted by various models, such as elliptical (elastic), cohesive zone (tapered profile in Fig. 7a), and linear. The reference values for average displacement and displacement area of the ideal shapes are as follows: elastic, $D_{avg} = 0.77$, $D_{area} = 1.57$; typical tapered profile (Walsh and Watterson, 1987), $D_{avg} = 0.52$, $D_{area} = 1.07$; and linear, $D_{avg} = 0.50$, $D_{area} = 1.00$.

Uncertainties in measuring the displacement distributions introduce some error into the normalized equivalents. For faults having $D_{max} = 100$ m, the measurement precision of ±2 m in elevation suggests that displacement values (D_{max}) vary within ±5%. Uncertainty in fault length centers on difficulties in precisely locating the zero-displacement point (M. Willemse, 1977, personal commun.), particularly where the faults exhibit long, gently tapering profiles such as in Devils Lane (Fig. 6; Schultz and Moore, 1996). For a typical graben such as Devils Lane, with $L = 4500$ m, a 100 m horizontal uncertainty in locating the fault tips leads to a change in length (to 4700 m) of only 0.1%. Alternatively, using the ±2 m vertical precision cutoff to "locate" the fault termination ($D \le 4$ m) contributes a horizontal uncertainty of perhaps 200 m, or <<1% of L. These uncertainties are sufficiently small that their influence on the shape comparison is not significant.

The two-dimensional shape parameters for Canyonlands faults are compared in Figure 7b with the ideal cases. Perfectly elastic displacement profiles would have elliptical shapes; every Canyonlands fault exhibits displacement-distribution shapes that are decidedly nonelliptical. The ramps formed near the ends of perfectly elastic faults would have steep dips (approaching 90°); in contrast, the ramps along Canyonlands faults (e.g., Fig. 6) are characterized by quite gentle dips (<10°: Trudgill and Cartwright, 1994), thus requiring an inelastic response of the jointed rock mass (Schultz, 1996) surrounding the fault (e.g., Schultz and Moore, 1996). Elastic profiles imply negligibly small end zones (length <<0.005L), large (singular) stress concentrations, and indefinitely strong rock at the fault terminations; none of these features would be expected for the joint surfaces observed beyond the faults. Tapered displacement profiles and gentle near-tip displacement gradients are consistent with those associated with localized slip along preexisting joints (e.g., Martel and Pollard, 1989) having relatively small shear strengths. Linear profiles may indicate variation in frictional properties as a function of displacement magnitude along the fault surface (Bürgmann et al., 1994). The nonelastic displacement profile shapes shown in Figure 7b suggest a broad range of possible cohesive-zone sizes that may span the entire fault length (Willemse, 1997).

The fault-shape data in Figure 7b reveal a range of tapers, with D_{avg}/D_{max} between 0.3 and 0.7. This range is influenced by fault-segment linkage. For example, the four individual faults of Devils Lane have $0.33 \le D_{avg}/D_{max} \le 0.51$ (Table 1). However, linkage of the eastern and western faults (Fig. 5) reduces the ratio, shifting the points to the lower left on the plot. The master faults in Devils Lane (ratios of 0.47 and 0.51) show a linked value of 0.44, whereas the antithetic one (individual ratios of 0.33 and 0.46) has a ratio of 0.32. Antithetic faults exhibit flatter displacement distributions than do the master faults regardless of whether the faults are considered to be discrete segments or linked. The dependence of D_{avg}/D_{max} on fault segment linkage may explain why several of the points in Figure 7b have such small ratios,

given that the faults are likely composed of several linked segments but are mapped as single faults (Trudgill and Cartwright, 1994).

We find a good correlation between average and maximum displacements for 11 Canyonlands faults, with $D_{avg}/D_{max} = 0.56 \pm 0.10$ ($n = 11$ faults). A comparable value ($D_{avg}/D_{max} = 0.62 \pm 0.06$, $n = 15$ faults) is reported for a population of smaller (24 m ≤ L ≤ 2210 m) normal faults in welded Bishop Tuff from Owens Valley, California (Dawers et al., 1993). Their data set also includes echelon segments and a fault composed of bridged echelon ("hard-linked") segments. The values of normalized average displacement, ~0.6, suggest tapered shapes for those fault-displacement distributions (Fig. 7). In both cases (Canyonlands and Bishop Tuff), the normal faults likely nucleated along preexisting joints, implying that the shapes of the displacement profiles associated with this process are similar, despite differences in rock type (welded tuff vs. jointed clastic rocks) and scale.

Comparison of displacement area, D_{area} (or, equivalently, average displacement), across opposing faults of the same graben permits quantification of the degree of cross-sectional symmetry of the graben-bounding faults. We define an asymmetry factor $F = (M - A)/M$, where M is D_{area} of the master fault (the greater D_{area} value) and A is that for the opposing fault (the lesser D_{area} value). For grabens whose faults have equal stratigraphic offsets and hence are perfectly symmetric, $F = 0$; asymmetric grabens have $F > 0$. Previous work noted only minor variations (i.e., ~10%) in displacement for graben faults (Trudgill and Cartwright, 1994) or suggested complete symmetry (McGill and Stromquist, 1979).

Our profiles reveal asymmetry factors approaching 40% across several grabens including Devils Lane, demonstrating a large degree of asymmetry in the geometry of Canyonlands grabens. Moreover, the differences in throw are consistent with other distinctive characteristics, such as rollover anticlines and footwall uplifts (discussed in a later section), that suggest that the kinematics and mechanics of normal faulting in the Canyonlands are better described by asymmetric-graben models (e.g., Rosendahl, 1987) rather than by symmetric, keystone-collapse models. Indeed, physical experiments by Ge and Jackson (1998) suggest that the geometry of faulting characteristic of Canyonlands grabens is inconsistent with the suite of normal and reverse faults associated with downward displacement of a "plug" in response to withdrawal of subjacent salt.

It is interesting that the degree of asymmetry is found to vary systematically with distance from the Colorado River (Fig. 8a). The easternmost graben used for this comparison, Devils Pocket, has an asymmetry factor F of 39%. This result is larger than the asymmetry factor F of 32% found for the Devils Lane graben system. Closer to the river, F decreases to 22% for Cyclone Canyon. The westernmost graben considered in this analysis is southeast Twin Canyon, where F is only 11%. The progression in graben asymmetry is superimposed on a previous separation of the Needles District grabens into two domains, based on "complexity" of graben structure: an inner domain close to Cataract Canyon (Fig. 3), defined in part by tilted beds between grabens, and an outer domain farther away, defined by a simpler pregraben stratigraphic sequence (Stromquist, 1976; McGill and Stromquist, 1979). Examination of the sense of graben asymmetry shows that the grabens within the inner domain typically have west-facing master faults, whereas the outer domain exhibits east-facing (counter-regional) master faults (Schultz and Moore, 1996; Fig. 8a). More complex grabens like those found in the inner domain (McGill and Stromquist, 1979; Schultz and Moore, 1996) have more symmetric cross-sectional geometry than the simpler, more asymmetric grabens in the outer domain. Although the specific mechanisms for these progressions remain to be clarified, the change in graben geometry is consistent with previous suggestions (McGill and Stromquist, 1979; Huntoon, 1982) that the grabens closer to the Colorado River are oldest and/or show the greatest amount of strain, resulting in a greater degree of symmetry (e.g., Rosendahl, 1987).

Figure 9. Along-strike view of southern Devils Lane graben, looking southwest, showing distinct differences in stratigraphic offset across graben. CM—dipping Cedar Mesa Sandstone block at south-dipping ramp in stepover between Devils Lane grabens. Note pickup truck near antithetic side of graben (below left arrow) for scale; graben width ~200 m. Compare to Figure 6.

The degree of graben asymmetry is not the only factor that varies across the strike of the graben array. Fault-slip data for the grabens along our traverse are listed in Table 2. We find that D_{max} also changes significantly as a function of distance from the Colorado River (Fig. 8b), decreasing with the ~5 km distance by about a factor of four. However, other parameters including fault length do not show such a correlation. We infer that older grabens in the Canyonlands are characterized by D_{max}/L ratios of 3×10^{-2} to 6×10^{-2} (data for the southeast and northwest faults bounding Twin Canyon graben, Table 2), whereas younger ones still accumulating displacement generally show smaller ratios (e.g., Devils Pocket, Table 2). The graben faults apparently maintain a displacement profile ($1 \times 10^{-2} < D_{max}/L < 6 \times 10^{-2}$) that shows moderate variations with increasing strain. These variations are likely related to the mechanical interaction between graben faults, which can enhance or impede lateral propagation for a given amount of displacement (e.g., Segall and Pollard, 1980; Aydin and Schultz, 1990; Willemse et al., 1996; Willemse, 1997), and to the systematic dependence of normal-fault geometry and linkage with increasing strain (as demonstrated by Cladouhos and Marrett, 1996).

Cross-Sectional Graben Geometry

Previous interpretations of the cross-sectional geometries of Canyonlands grabens were conceptual and schematic. Baars (1993, p. 98) inferred a down-to-the-west listric geometry for graben faults but curiously omitted the required tilting of surface rocks in his sketch. McGill and Stromquist (1979) inferred a symmetric geometry based on their interpretations of the near-surface structure and physical modeling studies. Using a modern framework of graben kinematics, Trudgill and Cartwright (1994) inferred that both graben faults may be listric, with one fault extending deeper toward the Paradox evaporites than the other. Cartwright et al. (1995, 1996) hypothesized that graben blocks sink into the Paradox evaporites as plugs. Our results using quantitative methods support the qualitative interpretation of Trudgill and Cartwright (1994) but extend beyond their suggestions by incorporating precise topography along with recent concepts of fault kinematics, reactive diapirs (Vendeville and Jackson, 1992), and area-balanced

Figure 10. South-facing aerial photograph shows differences in fault morphology (continuous and discontinuous fault traces) and throw along strike (throw is greater on the western fault, right-hand side of photograph) in Devils Lane graben width ~200 m. White rock on both sides of graben is Cedar Mesa Sandstone and is roughly planar at single-graben scale. S.O.B. Hill and ramp (Fig. 6) located at far end of road (toward top of photograph). Photograph by J. M. Moore.

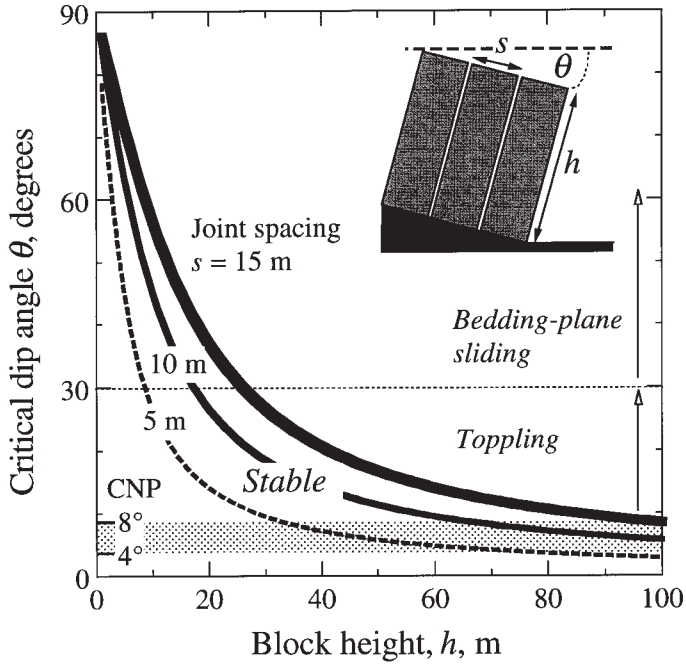

Figure 11. Plot showing the geometric conditions required for joint-bounded tilted blocks to rotate and fail by toppling. Inset defines geometry and parameters. Combinations of block height and tilt consistent with toppling (unstable) located to upper right of curves; stable tilted blocks (no toppling), below curves. Dashed horizontal line at 30° dip indicates approximate transition between toppling and, for steeper dips, bedding-plane sliding downdip. Typical stratal dips along graben walls, 4°–8°, suggest stability (no toppling) for blocks less than ~90 m high.

cross sections to provide testable predictions of the subsurface structure of the grabens.

We identify the following coherent assemblage of five characteristics for the grabens that demonstrate a clear asymmetric geometry in cross section (Schultz and Moore, 1996). These attributes, either individually or in concert, are persuasive indicators of asymmetric cross-sectional geometry, and they appear to apply to all grabens in the Canyonlands where the observations can be made.

1. There are significant differences in the amount of stratigraphic offset across asymmetric grabens (Fig. 9). These differential offsets, indicating master and antithetic faults, are documented in grabens that vary widely in size (e.g., Devils Pocket, Devils Lane, Cyclone Canyon, Red Lake Canyon).

2. The graben-bounding faults form a distinctive map pattern. The fault having greater stratigraphic offset (master fault) is continuous along the graben's length (Fig. 10), whereas that of the facing graben wall (antithetic fault) is discontinuous, segmented, and echelon.

3. Rollover anticlines formed adjacent to the antithetic fault appear related to the translation of strata down the master fault, resulting in local flexure (e.g., Higgs et al., 1991). An interesting related fact is that the widths of preexisting regional joints that parallel the graben also differ considerably across a graben: their greater widths (individual joint openings of perhaps several meters) on the antithetic side (Fig. 10) are associated with increased surface area and bending of the jointed rocks along the upper, outer surface of the rollover anticline.

4. Footwall uplift and gentle flexure, at least tens of meters in amplitude, occur adjacent to the master fault; these deformations decrease both along strike toward the fault terminations and across strike away from the fault trace. Preexisting joints are closed in the footwall area.

5. Preliminary seismic refraction results (Bush et al., 1996) demonstrate substantial floor tilt in northern Devils Lane graben, down toward the master fault and deeper (>65 m) in the center of the graben than near the ends (~15 m). The graben floor may be described as "spoon shaped," or deepest in the center and tilted down toward the master fault, beneath the overlying sedimentary wedge.

Tilted strata located in the hanging walls of the master graben faults dip into the graben at twice the regional slope (as steep as ~10°). Previous workers suggested that slab rotation and toppling into the graben-floor area was responsible for the stratal tilts (e.g., McGill and Stromquist, 1979; Trudgill and Cartwright, 1994). A simple kinematic analysis, however, demonstrates that toppling is not favored for most jointed slabs adjacent to graben walls. Toppling is governed by the relationship $\tan \theta = s/h$, where θ is the mini-

mum tilt angle, *s* is the characteristic joint spacing, and *h* is block height (West, 1995, pp. 291–296). If typical values of joint spacing *s* = 5–15 m and stratal tilts of 4°–8° are used, the relationship predicts that blocks up to 90 m in height will be stable against rotational failure into the graben (Fig. 11). Because most slabs on the antithetic sides of the grabens are less than 40 m in height, toppling is not considered to be an important or common mechanism for slab rotation. A hypothetical instance of toppling may occur early in the development of a graben, where very thin slabs might be rotated in association with flexure of the hanging wall due to slip on the master fault; if so, this process should occur before the formation of an antithetic fault. We note in passing that beds that dip into the graben interiors are found only on the antithetic sides or in ramps and stepovers; the restriction of dipping beds to one side of a graben is not explained by a model of topple failure into symmetric grabens (e.g., McGill and Stromquist, 1979).

Balanced cross sections, developed originally for regions dominated by thrust tectonics (e.g., Dahlstrom, 1969), are being used increasingly for extensional-tectonics problems, asymmetric grabens, and salt systems (Gibbs, 1984; Groshong, 1989; Jackson and White, 1989; Jackson and Vendeville, 1994; Roberts and Yielding, 1994). Rigorously balancing cross sections requires special techniques in regions of salt tectonics and evaporite flow (Schultz-Ela, 1992; Vendeville and Jackson, 1992; Jackson and Vendeville, 1994; Schultz-Ela and Jackson, 1996; Nalpas and Brun, 1993) that can render even balanced cross sections nonretrodeformable if salt migration into or out of the specific section is not also taken into account.

An area-balanced cross section has been constructed for the well-constrained southern end of northern Devils Lane graben (Fig. 12) located about 100 m north of S.O.B. Hill. Slip along the master fault is associated with deformation of the hanging wall, producing an extensional fault-bend fold (Groshong, 1989). The graben width of ~140 m is well predicted from the fault geometry by using the 80 m offset measured along the section line. We infer that slip along the master fault occurred first (allowing the use of Groshong's [1989] half-graben methodology), followed by nucleation and slip along the antithetic fault, consistent with observations and analyses of other grabens (e.g., Melosh and Williams, 1989; Vendeville and Jackson, 1992). The potential void created at depth due to small (~10 m) flexure of the footwall (Weissel and Karner, 1989)—as we and others (Trudgill and Cartwright, 1994) have observed in several grabens in Canyonlands and as implied by the fault offsets—is probably accommodated and filled by upward salt flow, producing an asymmetric reactive diapir (Vendeville and Jackson, 1992; Jackson et al., 1994) under the graben. The cross section predicts that the top of the underlying Paradox evaporites should be offset by ~40 m (the difference between the throws of the master fault and the antithetic fault) for this medium-sized graben.

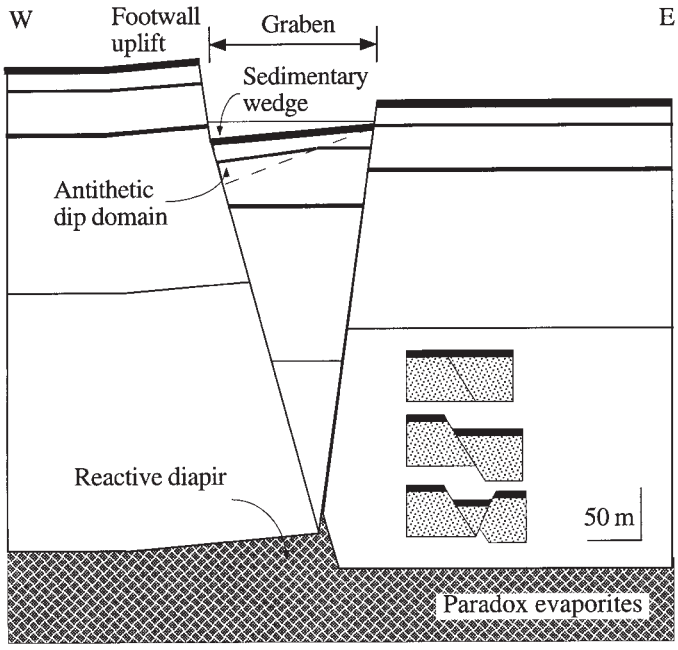

Figure 12. Balanced cross section for southern part of northern Devils Lane graben. Inset shows simplified deformation sequence (after Vendeville and Jackson, 1992) to incorporate slip along antithetic fault; slip along master (west) fault has been area-balanced following Groshong (1989). Master fault dip, 85° in upper 100 m, 75° down to Paradox evaporites; throw, 80 m; dipping beds on antithetic side define "fault-bend fold" due to master fault geometry; antithetic fault dips 80°. Horizontal reference line midway down in faulted section is approximate contact of Rico and upper Hermosa Formations; patterned region below is the Paradox Member.

A schematic cross section through the northern Needles District (Fig. 13) incorporates the precision topography along with the systematic facing direc-

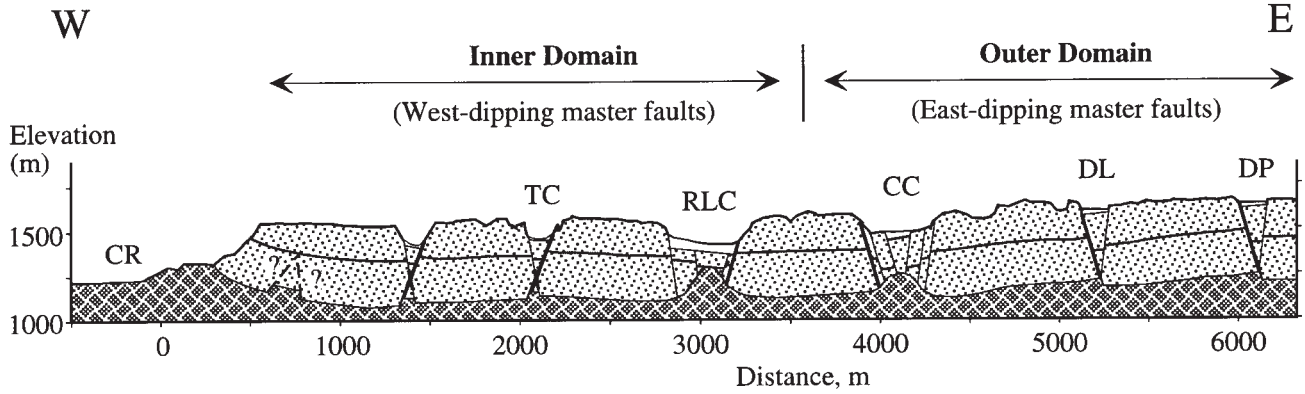

Figure 13. Schematic cross section through northern part of the Needles District graben system (Fig. 3). Reference line midway down in faulted section is approximate contact of Rico Formation and upper part of the Hermosa Formation; patterned region below is the Paradox Member of the Hermosa Formation. Note west-facing master faults in the inner domain, east-facing master faults in the outer domain. TC—southeast Twin Canyon; RLC—Red Lake Canyon; CC—Cyclone Canyon; DL—Devils Lane graben; DP—Devils Pocket graben; White—sedimentary graben fills; CR—Colorado River gorge and position of Meander anticline.

tions of the master faults. Larger grabens such as Cyclone Canyon or Red Lake Canyon may be underlain by much larger salt diapirs than the diapir beneath Devils Lane (Fig. 13), given their greater displacements (Vendeville and Jackson, 1992; see remarkably similar physical model results by McGill and Stromquist, 1979). Red Lake Canyon is sufficiently wide and deep that its subjacent salt diapir may be either reactive or active (as discussed in a later section), depending on the details of graben configuration and the thickness of sedimentary fill (Vendeville and Jackson, 1992; Schultz-Ela et al., 1993). The sedimentary section appears to be responding to extension over a viscous evaporite substrate by necking and boudinage (e.g., Johnson and Fletcher, 1994, p. 379–381; Triantafyllidis and Leroy, 1994), similar to the experimental results reported by McGill and Stromquist (1979). This behavior implies that the overall deformation mechanics of the necking plate (including its interaction with subjacent evaporites) may also be a contributing factor in the displacement distributions (Ely, 1987)—and thereby in the displacement vs. length scaling relationships—along the graben-bounding faults.

Extension and Strain Rate

Estimates of the amount of extension above the Paradox Member, or of the strain rate associated with graben faulting, have not been made previously to our work. Construction of topographic profiles normal to the grabens allows an estimation of the extension in the northern Needles District fault zone to be made (Schultz and Moore, 1996; Moore, 1997). Calculation of the throw and heave for each graben-bounding normal fault in a transect allows the comparison of the original and deformed length of the transect. Application of this process to a transect in the northern part of the Needles District suggests an original length of 5.18 km and a deformed length of 6.47 km. These values yield an extension of 25% along the transect [(6.47 – 5.18)/5.18].

The extension value can be combined with the suggested age of the grabens to determine a strain rate. Paucity of datable Quaternary materials makes age determination on the Colorado Plateau challenging (S. Olig and N. Biggar, 1996, 1997, personal commun.). The oldest sediment at the base of a swallow hole in an unnamed western graben was found to be 60–65 ka (Biggar, 1986; Biggar and Adams, 1987). This is considered to provide an estimate for the minimum age of the graben system, and the sediment was thought to have been deposited when about 25% of today's graben system had formed (Biggar, 1986). Use of this age produces a maximum strain rate because the grabens must be older than the sediment that fills them. The strain rate using this young date is about 10^{-13} s^{-1} [$0.25/(2.05 \times 10^{12}$ s)] or about 2 cm/yr [$(1.29 \times 10^{5}$ cm)/65 000 yr]. Biggar (1986) postulated an age of approximately 85 000 yr for the initiation of extension in the Needles District. Use of this age decreases the strain rate by less than an order of magnitude (10^{-14} s^{-1}) or to about 1.5 cm/yr.

The grabens are located within the Colorado Plateau, a region of moderately low natural earthquake activity (Wong et al., 1996). It is notable that the grabens as well as larger faults in the Paradox basin area such as the Moab fault (Olig et al., 1996) are aseismic (Wong et al., 1987). The only recorded activity between 1979 and 1986 in the Needles District was a cluster (February–March 1984) of 21 microearthquake events ($M_L \leq 1.8$) with hypocenters 6–10 km deep (Wong et al., 1987), which is far below the depth of Canyonlands grabens (~500 m). Faults in the region as large as those in the Canyonlands should normally produce earthquakes with magnitudes of $M_L \leq 4$–5 and repeat times of 100–200 yr (J. Moore, unpublished data, 1997; Wong et al., 1987, 1996).

The lack of seismicity along the faults has been attributed to their confinement to shallow crust by subjacent salt (e.g., Wong et al., 1996). This notion appears equivalent to stating that frictional sliding in the upper 500 m of the crust is stable (Marone and Scholz, 1988) with this creep-like behavior dependent on normal stress; rock, fault-zone, and rock-mass properties; slip-patch size; and environmental conditions (Scholz, 1990, p. 85–88). A full discussion of the stability of frictional sliding is beyond the scope of this paper. However, given the remarkably high strain rates implied for the district, if correct, we suggest that detailed studies of the Canyonlands grabens including Global Positioning System surveys may elucidate the mechanics of slip along these interesting structures, especially in the youngest, most asymmetric grabens and near stepovers where the maximum strain rates should occur.

Salt Tectonics

The Canyonlands grabens are comparable to other fault arrays produced in physical (Vendeville and Jackson, 1992; Childs et al., 1993; Nalpas and Brun, 1993; Guglielmo et al., 1997) and numerical (Schultz-Ela and Jackson, 1996) models of salt tectonics as well as documented field examples (Jackson and Vendeville, 1994; Jackson, 1995; Stewart et al., 1996). Common attributes include systematic fault spacing on the suprasalt cover (Schultz-Ela and Jackson, 1996), asymmetric graben geometry (e.g., Vendeville and Jackson, 1992; Childs et al., 1993; Nalpas and Brun, 1993; Schultz-Ela and Jackson, 1996; Jackson and Vendeville, 1994; Jackson et al., 1994; Stewart et al., 1996), and reactive diapirs or salt rollers below the grabens (McGill and Stromquist, 1979; Vendeville and Jackson, 1992; Childs et al., 1993; Stewart et al., 1996).

Extension of brittle strata in the Needles District produced asymmetric grabens that thinned the overburden and differentially loaded the salt, promoting the localization and ascent of reactive diapirs beneath the grabens (Jackson and Vendeville, 1994). Plausible rates of salt flow of >200 cm/yr (strain rates of 10^{-11} to 10^{-9} s^{-1}; Talbot and Rogers, 1980; Talbot and Jarvis, 1984; Jackson et al., 1994; M. Jackson, 1997, personal commun.) derived from salt glaciers far exceed the maximum rates of extension of the brittle sequence calculated above (strain rates of 10^{-13} to 10^{-14} s^{-1}), demonstrating that ductile salt deformation can easily keep pace with graben faulting. The transition from reactive diapirs, whose rise rate is controlled by the rate of crustal extension, to active diapirs, whose rise rate is controlled by the salt viscosity, can occur when the overburden is thinned by at least two-thirds to three-quarters of its original thickness (Vendeville and Jackson, 1992; Schultz-Ela et al., 1993). On the basis of the modeling results of Jackson and Vendeville (1994), salt diapirism below Devils Lane graben, which is ~100 m deep and ~200 m wide, is unequivocally reactive (Jackson and Vendeville, 1994, Fig. 9b). A 200-m-wide graben would need $D_{max} > 275$ m for salt diapirism below it to become active and intrude upward into the stratigraphy. Because D_{max} occurs either near fault midpoints or in the stepover regions between echelon faults (Fig. 5), the largest reactive diapirs should underlie these parts of the graben and decrease in amplitude along strike.

If the initiation of extension is assumed to be related to lateral unloading due to downcutting of the Colorado River (e.g., McGill and Stromquist, 1979; Huntoon, 1982)—and if a typical width of 1 km for the gorge with heights of ~360 m and ~530 m for the northern (near Lens Canyon) and southern (near Y Canyon) ends of the Needles District fault array, respectively, is used—then salt diapirism is predicted to be active in the north and formerly active, or emergent (salt exposed at the surface), in the south. This prediction is borne out by the exposures of Paradox evaporites to the south of Spanish Bottom but not to the north, near the study area (e.g., Potter and McGill, 1978). The critical overburden thickness for active diapirism to be initiated at the Colorado River is ~130 m, corresponding to the thickness of the Cedar Mesa Sandstone Member (of the Cutler Formation) and Rico Formation rocks (Stromquist, 1976). It appears that the active salt flow, the unloading and flexure of strata to form the Meander anticline (Harrison, 1927; Potter and McGill, 1978; Huntoon, 1982; Jackson and Vendeville, 1994), and the extension of the sequence to nucleate graben faults were begun where the river had carved down through much of the Permian section.

CONCLUSIONS

This research clarifies the structural geology of the Needles District fault zone and has direct implications for studies of the faulting process. We demonstrate that measurement of the full displacement profile along fault segments and use of two-dimensional shape parameters (i.e., D_{avg}, D_{area}) can provide information on rock mass and fault properties beyond that recovered by using only the maximum displacement. The consistent assemblage of characteristics defined for Canyonlands grabens that demonstrate an asymmetric cross-sectional form is applicable also to other grabens in different locations and tectonic regimes and having different scales. Variations in key parameters across the extensional province such as D_{max} demonstrate that displacement vs. length scaling relationships are sensitive to spatial gradients in the strain accommodated by graben faulting, with segment linkage being one manifestation of heterogeneous strain.

APPENDIX 1. STEREOPHOTOGRAMMETRIC DETAILS

Using the PG-2 stereoplotter allowed us to measure highly precise displacement profiles for the entire length of certain graben-bounding normal faults. We concentrated our efforts in the northern part of the Needles District fault zone for three reasons. First, the northern grabens are most accessible for field inspection and are most commonly discussed by other researchers. Second, focusing on one area limited the number of stereophotogrammetric models we were required to calibrate (a time-consuming process). Third, graben morphology is more clear than in the southern part of the field area where joints appear to die out (McGill and Stromquist, 1979). The Chesler lineament is roughly the southern boundary for our study. Data for our displacement profiles, along with values for maximum displacement, average displacement, and displacement area, are provided in Moore (1997).

Data acquired with the PG-2 are very precise (same value every measurement), but not necessarily accurate (measured value equals actual value) because our model is calibrated with the existing U.S. Geological Survey 7.5° topographic maps. Our absolute elevation measurements are diluted by National Mapping standards that only require spot elevations to be accurate to ±25% of the contour interval (J. Messerich, 1997, personal commun.). Published U.S. Geological Survey topographic quadrangles for the Needles District have 40 ft (~12 m) contour intervals that require spot elevations to be accurate to only ±3 m. This uncertainty produces stereo elevation models with high relative precision sufficient to discuss elevation differences, but the necessarily lower confidence in absolute accuracy complicates the integration of our data into an existing data set (i.e., a digital elevation model) without a correction factor. This correction is required to shift the elevation (*z*-axis) or tilt the reference plane (*x*- and *y*-axes) of the model to correct for absolute elevation errors. The absolute accuracy of our elevations is probably ±10 m (J. Messerich, 1996, 1997, personal commun.).

Our research focuses on the elevation differences between closely spaced points. We use the instrument to determine relative elevations between discrete points within the model (i.e., scarp height, displacements) and are therefore more concerned with relative precision than with absolute accuracy. Our relative precision in measurements of scarp relief and stratigraphic offsets in the study area, ±2 m, represents a significant improvement over previously published methods of estimating the scarp height that ranged from "dead reckoning" estimates of scarp heights to lowering a rope from the top of the scarp (B. Trudgill, 1996, personal commun.), in areas with poor access, to estimate the displacement.

With few exceptions, the topography in the Needles District is stratigraphically controlled (McGill and Stromquist, 1979), and in most cases, offset topography can be considered equivalent to offset stratigraphy (assuming that graben-filling sediments are relatively thin). An exception to this generalization is found in Cyclone Canyon where pregraben stratigraphy differs significantly across the graben (Schultz and Moore, 1996). This exception may be due to a preexisting structure (i.e., a fault or fold) or to a rollover anticline related to graben formation.

ACKNOWLEDGMENTS

Discussions in the field with George McGill, Eric Grosfils, Dan Schultz-Ela, and Simon Kattenhorn, and with Joe Cartwright, Bruce Trudgill, Manuel Willemse, Bill Higgs, Chuck Sword, Martin Jackson, Norma Biggar, Susan Olig, Richard Ely, Steve Wesnousky, Jaak Daemen, Jim Carr, Bob Watters, and Jim Messerich, led to significant refinements in the work reported here. Comments on the manuscript by Martin Jackson and Jenn Morgan and reviews by Mark Anders, Roland Bürgmann, and the Associate Editor improved the clarity of the presentation. Dick Hardyman and Jim Yount helped us with construction of the stereo models. Our work has benefited from informal discussions at the 1996 Paradox Basin Symposium, organized by Curt Huffman, and the American Association of Petroleum Geologists 1997 Hedberg Research Conference, organized by Bill Higgs and Chuck Kluth. We thank the members of the 1996 and 1997 Canyonlands Grabens Initiatives for their contributions in the field and personnel of the National Park Service for facilitating access to the grabens. We are also grateful to George McGill for his encouragement in studying the grabens. This work was supported in part by grants from NASA's Planetary Geology and Geophysics Program, the Mackay School of Mines, and Chevron Petroleum Technology Company.

REFERENCES CITED

Adhikary, D. P., Dyskin, A. V., Jewell, R. J., and Stewart, D. P., 1997, A study of the mechanism of flexural toppling failure of rock slopes: Rock Mechanics and Rock Engineering, v. 30, p. 75–93.

Anders, M. H., and Schlische, R. W., 1994, Overlapping faults, intrabasin highs, and the growth of normal faults: Journal of Geology, v. 102, p. 165–180.

Aydin, A., and Nur, A., 1985, The types and role of stepovers in strike-slip tectonics, *in* Biddle, K. T., and Christie-Blick, N., eds., Strike-slip deformation, basin formation, and sedimentation: Society of Economic Paleontologists and Mineralogists Special Publication 37, p. 35–44.

Aydin, A., and Schultz, R. A., 1990, Effect of mechanical interaction on the development of strike-slip faults with echelon patterns: Journal of Structural Geology, v. 12, p. 123–129.

Baars, D. L., 1962, Permian System of Colorado Plateau: American Association of Petroleum Geologists Bulletin, v. 46, p. 149–218.

Baars, D. L., 1993, Canyonlands country—Geology of Canyonlands and Arches National Parks: Salt Lake City, University of Utah Press, 138 p.

Baker, A. A., 1933, Geology and oil possibilities of the Moab District, Grand and San Juan Counties, Utah: U.S. Geological Survey Bulletin, 841, 95 p.

Banks, N. G., 1982, Set-up manual for orienting stereo models of aerial photographs on the Kern PG-2 photogrammetric plotter: U.S. Geological Survey Open File Report 82–985, 29 p.

Barnett, J. A. M., Mortimer, J., Rippon, J. H., Walsh, J. J., and Watterson, J., 1987, Displacement geometry in the volume containing a single normal fault: American Association of Petroleum Geologists Bulletin, v. 71, p. 925–937.

Biggar, N. E., 1986, Quaternary studies in the Paradox basin, southeastern Utah: Woodward-Clyde Consultants Topical Report, p. 86–87.

Biggar, N. E., and Adams, J. A., 1987, Dates derived from Quaternary strata in the vicinity of Canyonlands National Park, *in* Campbell, J. A., ed., Geology of Cataract Canyon and vicinity: Four Corners Geological Society, 10th Field Conference, Guidebook, p. 127–136.

Bruhn, R. L., and Schultz, R. A., 1996, Geometry and slip distribution in normal fault systems—Implications for mechanics and fault related hazards: Journal of Geophysical Research, v. 101, p. 3401–3412.

Bruhn, R. L., Yonkee, W. A., and Parry, W. T., 1990, Structural and fluid-chemical properties of seismogenic normal faults: Tectonophysics, v. 175, p. 130–157.

Bürgmann, R., Pollard, D. D., and Martel, S. J., 1994, Slip distributions on faults—Effects of stress gradients, inelastic deformation, heterogeneous host-rock stiffness, and fault interaction: Journal of Structural Geology, v. 16, p. 1675–1690.

Bush, N. I., Harris, C., and Grosfils, E. B., 1996, Refraction seismology in Devils Lane graben, Canyonlands National Park, Utah [abs.]: Eos (Transactions, American Geophysical Union), v. 77, p. F643.

Carter, K. E., and Winter, C. L., 1995, Fractal nature and scaling of normal faults in the Española basin, Rio Grande rift, New Mexico—Implications for fault growth and brittle strain: Journal of Structural Geology, v. 17, p. 863–873.

Cartwright, J. A., and Mansfield, C. S., 1998, Lateral displacement variation and lateral tip geometry of normal faults in the Canyonlands National Park, Utah: Journal of Structural Geology, v. 20, p. 3–19.

Cartwright, J. A., Trudgill, B. D., and Mansfield, C. S., 1995, Fault growth by segment linkage—An explanation for scatter in maximum displacement and trace length data from the Canyonlands grabens of SE Utah: Journal of Structural Geology, v. 17, p. 1319–1326.

Cartwright, J. A., Mansfield, C., and Trudgill, B., 1996, The growth of normal faults by segment linkage, *in* Buchanan, P. G., and Nieuwland, D. A., eds., Modern developments in structural interpretation, validation and modelling: Geological Society [London] Special Publication 99, p. 163–177.

Caskey, S. J., Wesnousky, S. G., Zhang, P., and Slemmons, D. B., 1996, Surface faulting of the 1954 Fairview Peak (M_s 7.2) and Dixie Valley (M_s 6.8) earthquakes, central Nevada: Seismological Society of America Bulletin, v. 86, p. 761–787.

Childs, C., Easton, S. J., Vendeville, B. C., Jackson, M. P. A., Lin, S. T., Walsh, J. J., and Watterson, J., 1993, Kinematic analysis of faults in a physical model of growth faulting above a viscous salt analogue: Tectonophysics, v. 228, p. 313–329.

Cladouhos, T. T., and Marrett, R., 1996, Are fault growth and linkage models consistent with power-law distributions of fault lengths?: Journal of Structural Geology, v. 18, p. 281–293.

Clark, R. M., and Cox, S. J. D., 1996, A modern regression approach to determining fault displacement-length relationships: Journal of Structural Geology, v. 18, p. 147–152.
Cowie, P. A., and Scholz, C. H., 1992a, Growth of faults by accumulation of seismic slip: Journal of Geophysical Research, v. 97, p. 11085–11095.
Cowie, P. A., and Scholz, C. H., 1992b, Displacement-length scaling relationship for faults: Data synthesis and discussion: Journal of Structural Geology, v. 14, p. 1149–1156.
Cowie, P. A., and Scholz, C. H., 1992c, Physical explanation for the length relationship of faults using a post-yield fracture mechanics model: Journal of Structural Geology, v. 14, p. 1133–1148.
Cowie, P. A., and Shipton, Z. K., 1998, On fault tip displacement gradients and process zone dimensions: Journal of Structural Geology, v. 20, p. 983–997.
Crider, J. G., and Pollard, D. D., 1998, Fault linkage—3D mechanical interaction between echelon normal faults: Journal of Geophysical Research, v. 103, p. 24373–24391.
Cruikshank, K. M., and Aydin, A., 1995., Unweaving the joints in Entrada Sandstone, Arches National Park, Utah, U.S.A.: Journal of Structural Geology, v. 17, p. 409–421.
Dahlstrom, C. D. A., 1969, Balanced cross sections: Canadian Journal of Earth Sciences, v. 6, p. 743–757.
Davison, I., 1994, Linked fault systems; extension, strike-slip and contractional, *in* Hancock, P. L., ed., Continental deformation: Pergamon, New York, p. 121–142.
Dawers, N. H., and Anders, M. H., 1995, Displacement-length scaling and fault linkage: Journal of Structural Geology, v. 17, p. 607–614.
Dawers, N. H., Anders, M. H., and Scholz, C. H., 1993, Growth of normal faults—Displacement-length scaling: Geology, v. 21, p. 1107–1110.
Ebinger, C. J., 1989, Geometric and kinematic development of border faults and accommodation zones, Kivu-Rusizi rift, Africa: Tectonics, v. 8, p. 117–133.
Elston, D. P., Shoemaker, E. M., and Landis, E. R., 1962, Uncompahgre front and salt anticline region of Paradox basin, Colorado and Utah: American Association of Petroleum Geologists Bulletin, v. 46, p. 1857–1878.
Ely, R. W., 1987, Colluvium-filled fault fissures in the Needles fault zone, Cataract Canyon, Utah, *in* Campbell, J. A., ed., Geology of Cataract Canyon and vicinity: Four Corners Geological Society, 10th Field Conference, Guidebook, p. 69–73.
Faulds, J. E., and Varga, R. J., 1998, The role of accommodation zones and transfer zones in the regional segmentation of extended terranes, *in* Faulds, J. E., and Stewart, J. H., eds., Accommodation zones and transfer zones—The regional segmentation of the Basin and Range province: Boulder, Colorado, Geological Society of America Special Paper 323 p. 1–45.
Gauthier, B., and Angelier, J., 1985, Fault tectonics and deformation—A method of quantification using field data: Earth and Planetary Science Letters, v. 74, p. 137–148.
Ge, H., and Jackson, M. P. A., 1998, Physical modeling of structures formed by salt withdrawal—Implications for deformation caused by salt dissolution: American Association of Petroleum Geologists Bulletin, v. 82, p. 228–250.
Gibbs, A. D., 1984, Structural evolution of extensional basin margins: Geological Society [London] Journal, v. 141, p. 609–620.
Groshong, R. H. Jr., 1989, Half-graben structures—Balanced models of extensional fault-bend folds: Geological Society of America Bulletin, v. 101, p. 96–105.
Gudmundsson, A., and Bäckström, K., 1991, Structure and development of the Sveinagja graben, northeast Iceland: Tectonophysics, v. 200, p. 111–125.
Guglielmo, G., Jr., Jackson, M. P. A., and Vendeville, B. C., 1997, Three-dimensional visualization of salt walls and associated fault systems: American Association of Petroleum Geologists Bulletin, v. 81, p. 46–61.
Harrison, T. E., 1927, Colorado-Utah salt domes: American Association of Petroleum Geologists Bulletin, v. 11, p. 111–133.
Higgs, W. G., Williams, G. D., and Powell, C. M., 1991, Evidence for flexural shear folding associated with extensional faults: Geological Society of America Bulletin, v. 103, p. 710–717.
Hunt, C. B., 1969, Geologic history of the Colorado River: U.S. Geological Survey Professional Paper 669–C, p. 59–130.
Huntoon, P. W., 1982, The Meander anticline, Canyonlands, Utah—An unloading structure resulting from horizontal gliding on salt: Geological Society of America Bulletin, v. 93, p. 941–950.
Huntoon, P. W., Billingsley, G. H., and Breed, W. J., 1982, Geologic map of Canyonlands National Park and vicinity, Utah: The Canyonlands Natural History Association, scale 1:62 500.
Jackson, J. A., and White, N. J., 1989, Normal faulting in the upper continental crust: Observations from regions of active extension: Journal of Structural Geology, v. 11, p. 15–36.
Jackson, M. P. A., 1995, Retrospective salt tectonics, *in* Jackson, M. P. A., Roberts, D. G., and Snelson, S., eds., Salt tectonics—A global perspective: American Association of Petroleum Geologists Memoir 65, p. 1–28.
Jackson, M. P. A., and Vendeville, B. C., 1994, Regional extension as a geologic trigger for diapirism: Geological Society of America Bulletin, v. 106, p. 57–73.
Jackson, M. P. A., Vendeville, B. C., and Schultz-Ela, D. D., 1994, Structural dynamics of salt systems: Annual Review of Earth and Planetary Sciences, v. 22, p. 93–117.
Johnson, A. M., and Fletcher, R. C., 1994, Folding of viscous layers: New York, Columbia University Press, 461 p.
Larsen, P. H., 1988, Relay structures in a Lower Permian basement-involved extension system, east Greenland: Journal of Structural Geology, v. 10, p. 3–8.
Lewis, R. Q., Sr., and Campbell, R. H.,1965, Geology and uranium deposits of Elk Ridge and vicinity, San Juan County, Utah: U.S. Geological Survey Professional Paper 474–B, 69 p.
Loope, D. B., 1984, Eolian origin of upper Paleozoic sandstones, southeastern Utah: Journal of Sedimentary Petrology, v. 54, p. 563–580.
Loope, D. B., 1985, Episodic deposition and preservation of eolian sands—A late Paleozoic example from southeastern Utah: Geology, v. 13, p. 73–76.
Mack, G. H., and Seager, W. R., 1995, Transfer zones in the southern Rio Grande rift: Geological Society [London] Journal, v. 152, p. 551–560.
Marone, C., and Scholz, C. H., 1988, The depth of seismic faulting and the upper transition from stable to unstable regimes: Geophysical Research Letters, v. 15, p. 621–624.
Marrett, R., and Allmendinger, R. W., 1990, Kinematic analysis of fault-slip data: Journal of Structural Geology, v. 12, p. 973–986.
Martel, S. J., 1990, Formation of compound strike-slip fault zones, Mount Abbot quadrangle, California: Journal of Structural Geology, v. 12, p. 869–882.
Martel, S. J., 1997, Effects of cohesive zones on small faults and implications for secondary fracturing and fault trace geometry: Journal of Structural Geology, v. 19, p. 835–847.
Martel, S. J., and Boger, W. A., 1998, Geometry and mechanics of secondary fracturing around small three-dimensional faults: Journal of Geophysical Research, v. 103, p. 21299–21314.
Martel, S. J., and Pollard, D. D., 1989, Mechanics of slip and fracture along small faults and simple strike-slip fault zones in granitic rock: Journal of Geophysical Research, v. 94, p. 9417–9428.
McGill, G. E., and Stromquist, A. W., 1974, A model for graben formation by subsurface flow—Canyonlands National Park, Utah: Amherst, University of Massachusetts, Department of Geology and Geography Contribution 15, 79 p.
McGill, G. E., and Stromquist, A. W., 1975, Origin of graben in the Needles District, Canyonlands National Park, Utah, *in* Fassett, J. E., ed., Canyonlands country: Four Corners Geological Society, 8th Field Conference, Guidebook, p. 235–243.
McGill, G. E., and Stromquist, A. W., 1979, The grabens of Canyonlands National Park, Utah—Geometry, mechanics, and kinematics: Journal of Geophysical Research, v. 84, p. 4547–4563.
Melosh, H. J., and Williams, C. A., Jr., 1989, Mechanics of graben formation in crustal rocks—A finite element analysis: Journal of Geophysical Research, v. 94, p. 13961–13973.
Messerich, J. A., 1989, Shortcut method for photogrammetric setups on the PG-2 plotter: U.S. Geological Survey Rough Draft, 44 p.
Molenaar, C. M., 1987, Mesozoic rocks of Canyonlands country, *in* Campbell, J. A., ed., Geology of Cataract Canyon and vicinity: Four Corners Geological Society, 10th Field Conference, Guidebook, p. 19–24.
Moore, J. M., 1997, Displacement-length scaling, kinematics and mechanical implications of Canyonlands National Park grabens [master's thesis]: Reno, University of Nevada, 76 p.
Morley, C. K., Nelson, R. A., Patton, T. L., and Munn, S. G., 1990, Transfer zones in the East African rift system and their relevance to hydrocarbon exploration in rifts: American Association of Petroleum Geologists Bulletin, v. 74, p. 1234–1253.
Moustafa, A. R., 1997, Controls on the development and evolution of transfer zones—The influence of basement structure and sedimentary thickness in the Suez rift and Red Sea: Journal of Structural Geology, v. 19, p. 755–768.
Nalpas, T., and Brun, J.-P., 1993, Salt flow and diapirism related to extension at crustal scale: Tectonophysics, v. 228, p. 349–362.
Nuckolls, H. M., and McCulley, B. L., 1987, Origin of saline springs in Cataract Canyon, Utah, *in* Campbell, J. A., ed., Geology of Cataract Canyon and vicinity: Four Corners Geological Society, 10th Field Conference, Guidebook, p. 193–199.
Olig, S. S., Fenton, C. H., McCleary, J., and Wong, I. G., 1996, The earthquake potential of the Moab fault, and its relation to salt tectonics in the Paradox basin, Utah, *in* Huffman, A. C., Jr., Lund, W. R., and Godwin, L. H., eds., Geology and resources of the Paradox basin: Utah Geological Association Guidebook, v. 25, p. 251–264.
Peacock, D. C. P., and Sanderson, D. J., 1994, Geometry and development of relay ramps in normal fault systems: American Association of Petroleum Geologists Bulletin, v. 78, p. 147–165.
Peacock, D. C. P., and Sanderson, D. J., 1996, Effects of propagation rate on displacement variations along faults: Journal of Structural Geology, v. 18, p. 311–320.
Pickering, G., Peacock, D. C. P., Sanderson, D. J., and Bull, J. M., 1997, Modeling tip zones to predict the throw and length characteristics of faults: American Association of Petroleum Geologists Bulletin, v. 81, p. 82–99.
Pollard, D. D., and Aydin, A., 1988, Progress in understanding jointing over the past century: Geological Society of America Bulletin, v. 100, p. 1181–1204.
Pollard, D. D., and Segall, P., 1987, Theoretical displacements and stresses near fractures in rock—With applications to faults, joints, dikes, and solution surfaces, *in* Atkinson, B. K., ed., Fracture mechanics of rock: New York, Academic Press, p. 277–349.
Potter, D. B., Jr., and McGill, G. E., 1978, Valley anticlines of the Needles District, Canyonlands National Park, Utah: Geological Society of America Bulletin, v. 89, p. 952–960.
Roberts, A., and Yielding, G., 1994, Continental extensional tectonics, *in* Hancock, P. L., ed., Continental deformation: Pergamon, New York, p. 223–250.
Rosendahl, B. R., 1987, Architecture of continental rifts with special reference to East Africa: Annual Review of Earth and Planetary Sciences, v. 15, p. 445–503.
Schlische, R. W., Young, S. S., Ackermann, R. V., and Gupta, A., 1996, Geometry and scaling relations of a population of rift-related normal faults: Geology, v. 24, p. 683–686.
Scholz, C. H., 1990, The mechanics of earthquakes and faulting: New York, Cambridge University Press, 439 p.
Scholz, C. H., Dawers, N. H., Yu, J.-Z., and Anders, M. H., 1993, Fault growth and fault scaling laws—Preliminary results: Journal of Geophysical Research, v. 98, p. 21951–21961.
Schultz, R. A., 1996, Relative scale and the strength and deformability of rock masses: Journal of Structural Geology, v. 18, p. 1139–1149.
Schultz, R. A., 1997, Displacement-length scaling for terrestrial and Martian faults—Implications for Valles Marineris and shallow planetary grabens: Journal of Geophysical Research, v. 102, p. 12009–12015.
Schultz, R. A., and Moore, J. M., 1996, New observations of grabens from the Needles District, Canyonlands National Park, Utah, *in* Huffman, A. C., Jr., Lund, W. R., and Godwin, L. H., eds., Geology and resources of the Paradox basin: Utah Geological Association Guidebook, v. 25, p. 295–302.
Schultz-Ela, D. D., 1992, Restoration of cross sections to constrain deformation processes of ex-

tensional terranes: Marine and Petroleum Geology, v. 9, p. 372–388.
Schultz-Ela, D. D., and Jackson, M. P. A., 1996, Relation of subsalt structures to suprasalt structures during extension: American Association of Petroleum Geologists Bulletin, v. 80, p. 1896–1924.
Schultz-Ela, D. D., Jackson, M. P. A., and Vendeville, B. C., 1993, Mechanics of active salt diapirism: Tectonophysics, v. 228, p. 275–312.
Segall, P., and Pollard, D. D., 1980, Mechanics of discontinuous faults: Journal of Geophysical Research, v. 85, p. 4337–4350.
Stevenson, G. M., and Baars, D. L., 1986, The Paradox—A pull-apart basin of Pennsylvanian age, *in* Peterson, J. A., ed., Paleotectonics and sedimentation in the Rocky Mountain region, United States: American Association of Petroleum Geologists Memoir 41, p. 513–539.
Stewart, S. A., Harvey, M. J., Otto, S. C., and Weston, P. J., 1996, Influence of salt on fault geometry—Examples from the UK salt basins, *in* Alsop, G. I., Blundell, D. J., and Davison, I., eds., Salt tectonics: Geological Society [London] Special Publication 100, p. 175–202.
Stromquist, A. W., 1976, Geometry and growth of grabens, lower Red Lake Canyon area, Canyonlands National Park, Utah: Amherst, University of Massachusetts, Department of Geology and Geography Contribution 28, 118 p.
Talbot, C. J., and Jarvis, R. J., 1984, Age, budget and dynamics of an active salt extrusion in Iran: Journal of Structural Geology, v. 6, p. 521–533.
Talbot, C. J., and Rogers, E. A., 1980, Seasonal movements in a salt glacier in Iran: Science, v. 208, p. 395–397.
Triantafyllidis, N., and Leroy, Y. M., 1994, Stability of a frictional material layer resting on a viscous half-space: Mechanics and Physics of Solids Journal, v. 42, p. 51–110.
Trudgill, B., and Cartwright, J., 1994, Relay-ramp forms and normal-fault linkages, Canyonlands National Park, Utah: Geological Society of America Bulletin, v. 106, p. 1143–1157.
Vendeville, B. C., and Jackson, M. P. A., 1992, The rise of diapirs during thin-skinned extension: Marine and Petroleum Geology, v. 9, p. 331–353.
Walsh, J. J., and Watterson, J., 1987, Distributions of cumulative displacement and seismic slip on a single normal fault surface: Journal of Structural Geology, v. 9, p. 1039–1046.
Weissel, J. K., and Karner, G. D., 1989, Flexural uplift of rift flanks due to mechanical unloading of the lithosphere during extension: Journal of Geophysical Research, v. 94, p. 13919–13950.
West, T. R., 1995, Geology applied to engineering: Englewood Cliffs, New Jersey, Prentice-Hall, 560 p.
Willemse, E. J. M., 1997, Segmented normal faults—Correspondence between three-dimensional mechanical models and field data: Journal of Geophysical Research, v. 102, p. 675–692.
Willemse, E. J. M., and Pollard, D. D., 1998, On the orientation and pattern of wing cracks and solution surfaces at the tips of a sliding flaw or fault: Journal of Geophysical Research, v. 103, p. 2427–2438.
Willemse, E. J. M., Pollard, D. D., and Aydin, A., 1996, Three-dimensional analyses of slip distributions on normal fault arrays with consequences for fault scaling: Journal of Structural Geology, v. 18, p. 295–309.
Witkind, I. J., 1994, The role of salt in the structural development of central Utah: U.S. Geological Survey Professional Paper 1528, 145 p.
Wong, I. G., Humphrey, J. R., Kollmann, A. C., Munden, B. B., and Wright, D. D., 1987, Earthquake activity in and around Canyonlands National Park, Utah, *in* Campbell, J. A., ed., Geology of Cataract Canyon and vicinity: Four Corners Geological Society, 10th Field Conference, Guidebook, p. 51–58.
Wong, I. G., Olig, S. S., and Bott, J. D. J., 1996, Earthquake potential and seismic hazards in the Paradox basin, southeastern Utah, *in* Huffman, A. C., Jr., Lund, W. R., and Godwin, L. H., eds., Geology and resources of the Paradox basin: Utah Geological Association Guidebook, v. 25, p. 241–250.

MANUSCRIPT RECEIVED BY THE SOCIETY JULY 17, 1997
REVISED MANUSCRIPT RECEIVED JUNE 25, 1998
MANUSCRIPT ACCEPTED AUGUST 4, 1998

Printed in U.S.A.